TECHNICAL REPORT

An effective approach for accurate estimation of VLBI–GNSS local-tie vectors

Saho Matsumoto[*] , Haruka Ueshiba, Tomokazu Nakakuki, Yu Takagi, Kyonosuke Hayashi, Toru Yutsudo, Katsuhiro Mori, Yudai Sato and Tomokazu Kobayashi

Abstract

The local-tie vectors, which connect coordinate frames of different space geodetic techniques, are indispensable for the construction of the International Terrestrial Reference Frame (ITRF). To obtain the local-tie vector connecting very long baseline interferometry (VLBI) sites with high measurement accuracy, it is crucial to accurately determine the antenna invariant point (IVP), which does not change its position under any tracking conditions. In the 2018 co-location survey at Ishioka station, we employed two methods to determine the IVP; "inside" and "outside" methods. We observed a target mirror from inside or outside of the antenna and derived trajectories of the target used for estimation of the rotation axes. Both the methods successfully estimated the IVPs with the measurement error of less than 1 mm, meeting the requirement of measurement accuracy by the International Earth Rotation and Reference Systems Service (IERS). The striking point is that the difference between the IVP positions was less than 1 mm, suggesting that both the methods could determine almost the same position independently. While they both can determine the IVPs with high measurement accuracy, it should be noted that the inside method substantially improved the operational efficiency. For the outside method, we had to repeat the target observations from four or more pillars around the VLBI antenna, with the reinstallation of a total station (TS) if needed. In contrast, for the inside method, we can observe the target from one place inside the antenna in a short time with only one TS no matter where the mirror is attached in the azimuth cabin. We concluded that the inside method is an effective and practical approach to accurately estimate the IVP.

Keywords: Local-tie vector, Co-location, Very Long Baseline Interferometry (VLBI), Invariant point, Inside method, Outside method

*Correspondence: matsumoto-s96n2@mlit.go.jp

Geospatial Information Authority of Japan, 1 Kitasato, Tsukuba, Ibaraki 305-0811, Japan

Matsumoto *et al. Earth, Planets and Space*   (2022) 74:147

Page 2 of 14

Graphical Abstract
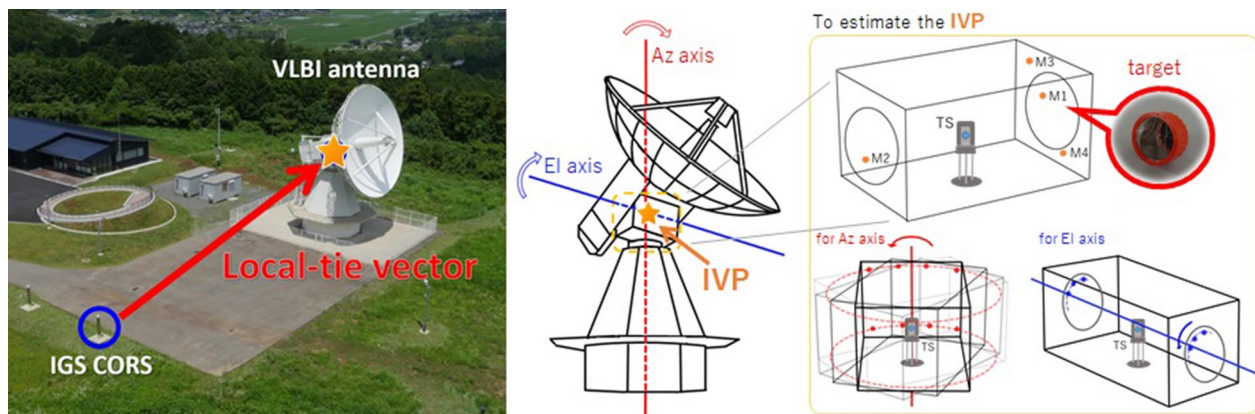
Introduction

The Global Geodetic Reference Frame (GGRF) is a fundamental and inevitable platform to know a common position. One of the most well-known GGRFs is the International Terrestrial Reference Frame (ITRF) provided by International Earth Rotation and Reference Systems Service (IERS) (https://www.iers.org/IERS/EN/DataProducts/ITRF/itrf.html). The ITRF is constructed with four space geodetic techniques: Global Navigation Satellite System (GNSS), Satellite Laser Ranging (SLR), Doppler Orbitography and Radiopositioning Integrated by Satellite (DORIS), and Very Long Baseline Interferometry (VLBI) (Petit and Luzum 2010; Altamimi et al. 2016, 2017). The TRF solutions of station coordinates are individually determined by each technique, and this is why they are spatially independent of one another, resulting in a spatial inconsistency. Therefore, it is essential to combine the solutions to construct one frame, namely, the ITRF. The information on relative positions to tie the different frames is known as local-tie vectors (Altamimi 2008). The survey to determine the local-tie is called co-location. The quality of the local-tie should be directly related to that of the ITRF; therefore, it is crucial to conduct the co-location with high accuracy as well as with individual space geodetic observations.

Ishioka Geodetic Observing Station (hereafter called Ishioka) is one of the co-location sites (Altamimi 2005; Rothacher et al. 2009) in Japan, where VLBI and GNSS sites are located (Fig. 1). To measure the local-tie between VLBI and GNSS, it is required to determine the reference position of the VLBI antenna, which is the invariant point of antenna (hereafter referred to as IVP). However, it is not so easy to determine the IVP, because the IVP is positioned "somewhere" in the antenna structure, i.e.,

the position is invisible and inaccessible. In the background, the methods to indirectly estimate the IVP have been developed (Woods 2008). The methods are categorized into two types in this study, inside method and outside method. In the outside method, a target mirror
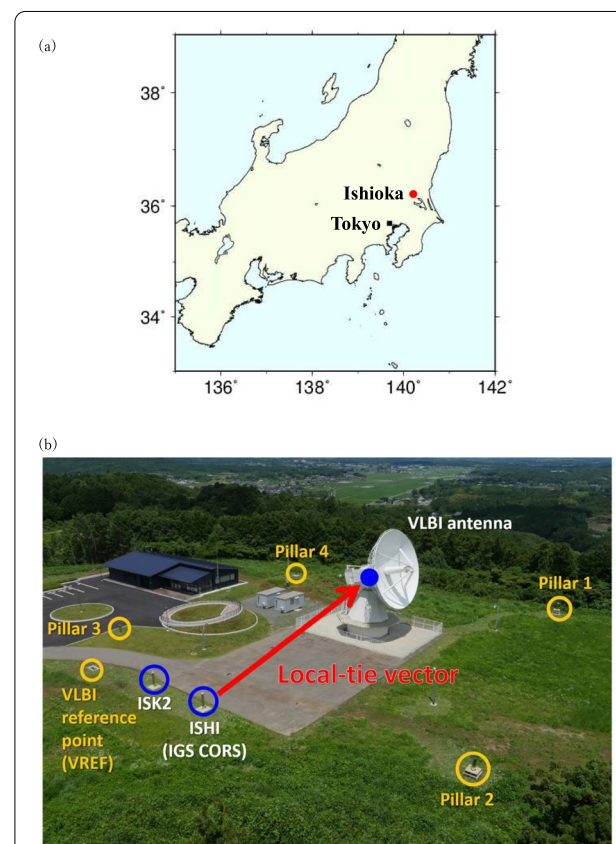

Fig. 1 Location and the panoramic view of the Ishioka station. **a** Location map; **b** panoramic view

Matsumoto *et al. Earth, Planets and Space* (2022) 74:147

Page 3 of 14

is measured, which is used to estimate the IVP, from the outside of the VLBI antenna, while in the inside method, the target is measured from the inside of the antenna. The outside method is applicable to any type of antenna structure and is one of the conventional ways to estimate the IVP (Hasegawa et al. 2002). However, this method is time-consuming and laborious, because it is necessary to observe the target from various directions while changing locations. On the other hand, the inside method is a novel approach for the estimation of IVP as we can conduct the survey efficiently in a short time, although it is allowed for the antenna to have a specific structure containing the pillar inside (López-Ramasco and Córdoba-Hita 2017). If the inside method achieves the measurement accuracy level desired by IERS, it can improve the efficiency of co-location. However, there is little documentation on how accurately the inside method can estimate the local-ties compared with the outside method. With this background, we applied both the methods at the same station to confirm whether the inside method can be used as an alternative to estimate the IVP.

In this paper, first, we will introduce the method of VLBI–GNSS local-tie survey in Ishioka and describe two methods for the estimation of IVP. Second, we will show the results of co-location that took place in 2018, using both the methods, and compare the measurement accuracy and the operational efficiency.

Co-location at Ishioka

Ishioka is located in Ibaraki prefecture of Japan (Fig. 1a), about 70 km from Tokyo, and is operated by the Geospatial Information Authority of Japan (GSI). This station has two space geodetic observation systems: VLBI and GNSS. A 13.2 m radio telescope is installed in the station, and GSI has been participating in international observations coordinated by International VLBI Service (IVS) since 2015. It is the first antenna in Japan meeting the criteria for "VLBI Global Observing System (VGOS)", which aims to achieve high precision results by high-speed operation of the antenna, wide bandwidth observation, and high-speed network connection (Petrachenko et al. 2009). The GNSS station "ISHI" is registered by the International GNSS Service (IGS) as an IGS Continuously Operating Reference Station (CORS) and has provided the GNSS data continuously. The data obtained from these sites play an essential role in the ITRF construction. Therefore, Ishioka station is one of the most important sites for the global geodetic survey.

Figure 1b shows the panoramic view of Ishioka station. The local-tie obtained by the co-location is the vector between the IVP of the VLBI antenna and the GNSS antenna reference point, which is drawn with a red arrow. To determine the local-tie, four pillars

(numbered 1, 2, 3, and 4) are placed around the VLBI antenna and the GNSS antenna. In addition, there is a ground marker for VLBI, which does not have the global coordinate and is meant for domestic use only. All these points have DOMES (Directory of MERIT Sites) numbers registered by IERS Additional file 1: (Table S1).

Method for estimate of IVP

Outline of co-location

IERS requires the estimation of the local-tie within 1 mm accuracy (Poyard 2017). To achieve this, traditional survey methods such as traversing and levelling are competent.

The process of co-location is roughly divided into two processes; one is a survey to measure a local-tie in a local frame (Fig. 2a), and the other is to unite a coordinate in a local frame to a global frame (Fig. 2b). First, we determine the VLBI–GNSS local-tie in the local frame. The antenna reference point (hereafter called ARP) of the GNSS is defined as the center of the bottom of the choke ring antenna's ground plane. Since we cannot measure the endpoints of local-tie, we conducted the survey in the following three steps:
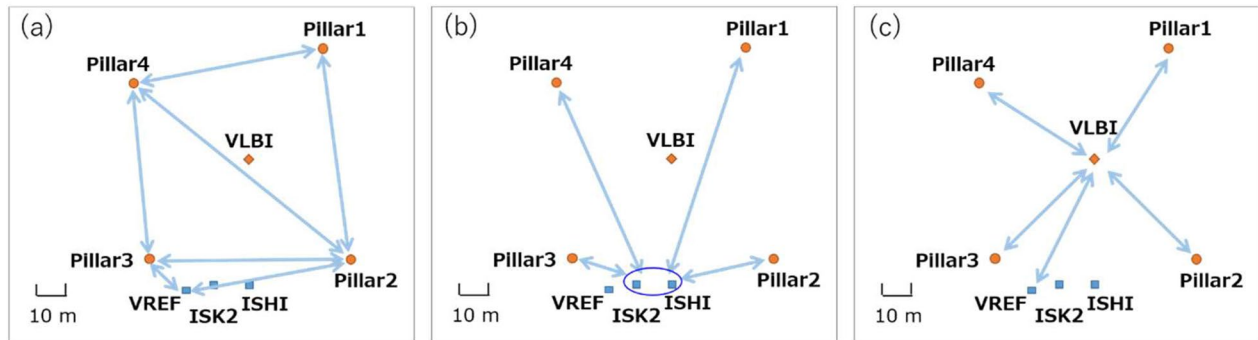
(a) Measuring the positional relation of pillars,
(b) Measuring the positional relation between pillars and ARP, and
(c) Measuring the positional relation between pillars and IVP.

These surveys were conducted in combination with traversing and levelling surveys. Through the three steps, VLBI and GNSS were connected in the local frame. In the next step, we measured orientation angles to rotate the coordinates of the local frame to the global frame using Total Station (TS) and GNSS (Fig. 2b). Moreover, correction of vertical deviation was required to unite Geocentric Coordinate System conforming to ITRF. The main aim of this study, which is identify the method of measuring the relationship between the pillars and VLBI antenna, is described in next section. The details of the other surveys are described in Additional file 5: (Text S1).

Observation methods to determine rotation axes

We focused on the methods of estimation of the IVP that is indispensable to obtain a local-tie. The Ishioka's VLBI antenna has azimuth and elevation (hereafter called Az and El, respectively) mounting types that the antenna rotates in Az and El directions around the axes. The IVP is sometimes defined as "secondary axis projection over the primary axis" (Dawson et al. 2005; Poyard 2017), where primary and secondary axes are equivalent to Az

Matsumoto *et al. Earth, Planets and Space*   (2022) 74:147
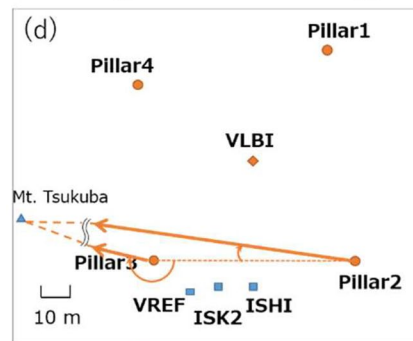
Page 4 of 14

Fig. 2 Outline of co-location survey. **a** Measuring the positional relations of pillars; **b** measuring the positional relations between pillars and ARP of GNSS; **c** measuring the positional relations between pillars and IVP of VLBI; **d** measuring the orientation angle

and El axes on Az and El mounting type antenna, including Ishioka; hereinafter it is simply defined as the intersection of the Az axis and the El axis (Fig. 3a). The Az and El axes can be individually estimated using trajectories of a fixed point on the antenna. To obtain the trajectory data, we installed a target mirror attached to the antenna as the fixed point and estimated the position of the target by measuring the distance and the angle between the target and a pillar, where a TS is installed. Each time the measurement was completed, we rotated the antenna around the El axis and measured the target position again. By repeating the measurements, we acquired one data set to estimate the El axis (blue dots in Fig. 3a). After obtaining the data set for one El axis, we rotated the antenna around the Az axis and repeated the measurements for various elevation angles in the same manner. By repeating the measurements by rotating the antenna around the Az axis, we collected the data set to estimate the Az axis (red dots in Fig. 3a). Using the trajectory data for the El and the Az axes, we determined the positions of the El and the Az axes using the least squares approach.

The measurement of the IVP position is one of the potential sources that produces relatively large errors

in the co-location survey, as the invisible IVP position cannot be directly measured. Therefore, it is crucial to accurately measure the target positions for the accurate determination of IVP position. For this purpose, there are two methods to measure the target positions; the outside method and the inside method. In general, antenna thermal expansion could affect the estimation of IVP. However, the issue concerning the thermal effect is beyond the scope of this study, and needs extensive study in future.

Outside method
In the outside method, we observed the target mirror from the "outside of the antenna structure". The target mirror was attached to the outside wall of the antenna moving part (Fig. 4). This target was observed at neighboring pillars with TSs installed on the pillars. Once we had measured the distance and angle from the pillars, we moved the antenna around the El axis, and observed the target mirror again. We repeatedly observed several elevation angles with a constant azimuth direction. After the measurement, we rotated the antenna around the Az axis and made similar observations for various elevation
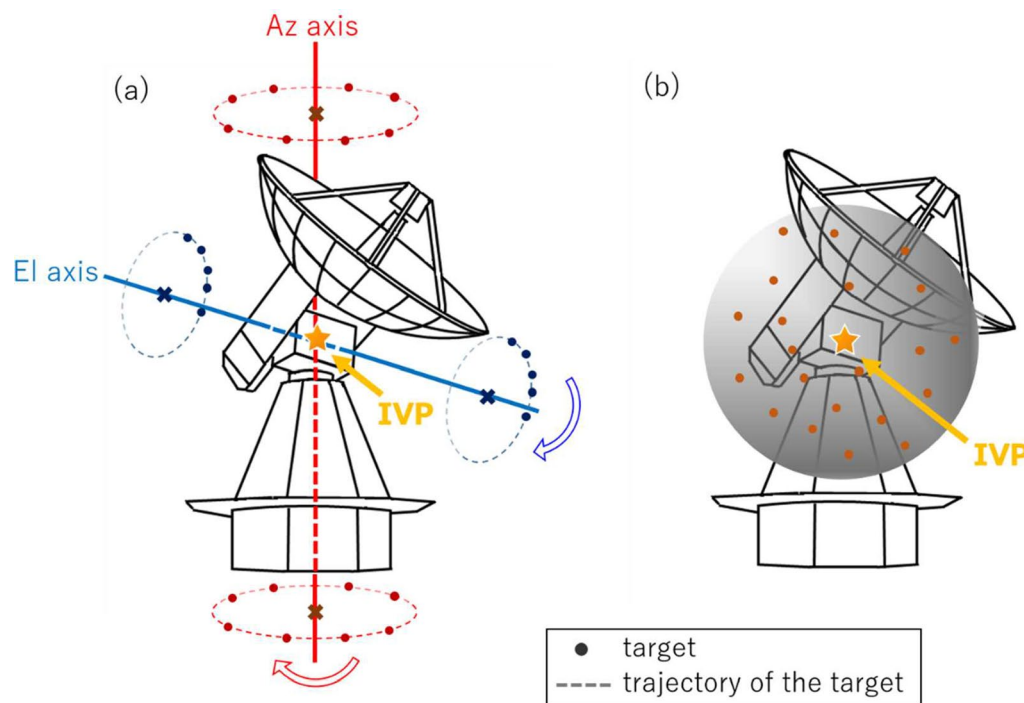
Matsumoto *et al. Earth, Planets and Space*   (2022) 74:147

Page 5 of 14

Fig. 3 Conceptual picture of how to estimate IVP. **a** Relation between rotation axes, IVP and target positions for axis method. El and Az axes are estimated with target positions indicated by blue and red dots, respectively; **b** relation between IVP and target positions for sphere method
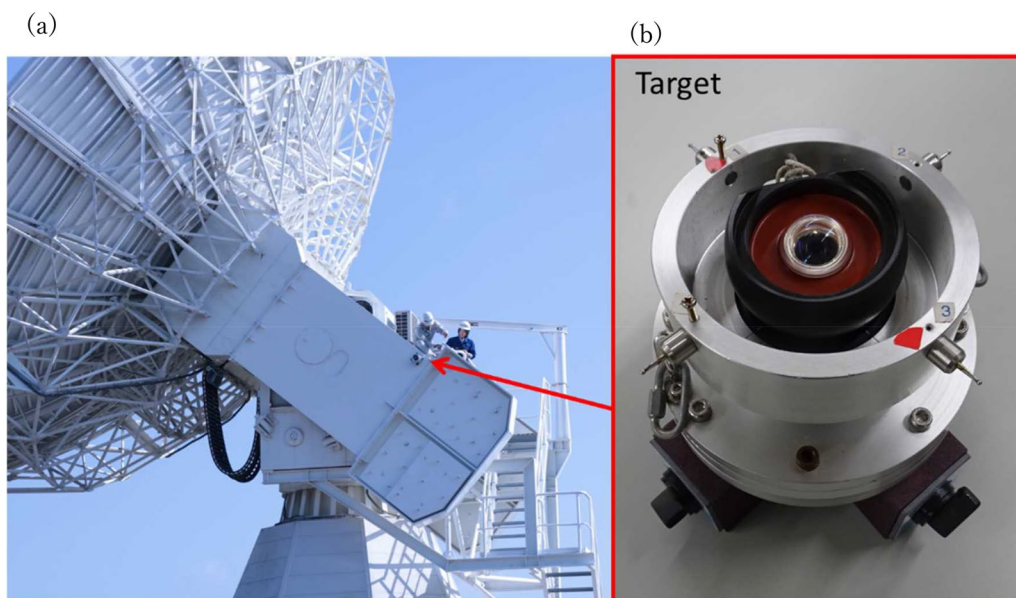

Fig. 4 Target for outside method. **a** Position attaching target mirror; **b** target mirror used for outside method (Cateye-reflector)

angles. There could be a maximum of two pillars from which a target can be directly measured. After rotating the antenna around the Az axis, we observed the target at other pillars, where target was hidden behind and was not visible.

Matsumoto *et al. Earth, Planets and Space*   (2022) 74:147

Page 6 of 14

The observed points were distributed on a circular arc around an axis (Fig. 3a). From a series of observations, we drew arcs from the target's trajectory and estimated one axis corresponding to the center points of these arcs by the least squares method. We could finally determine the IVP from the intersection of the estimated El and Az axes.

Inside method

In the inside method, the target mirror is observed from the "inside of the antenna structure". The Ishioka's antenna has a specific structure, where a tall pillar reaching the Az cabin (Fig. 5) is installed inside the antenna (hereafter called inside pillar). Notably, the inside pillar is fixed on the ground and is independent of the antenna rotation. The target is observed not from the Pillars 1 to 4 (Fig. 1), but from the inside pillar only.
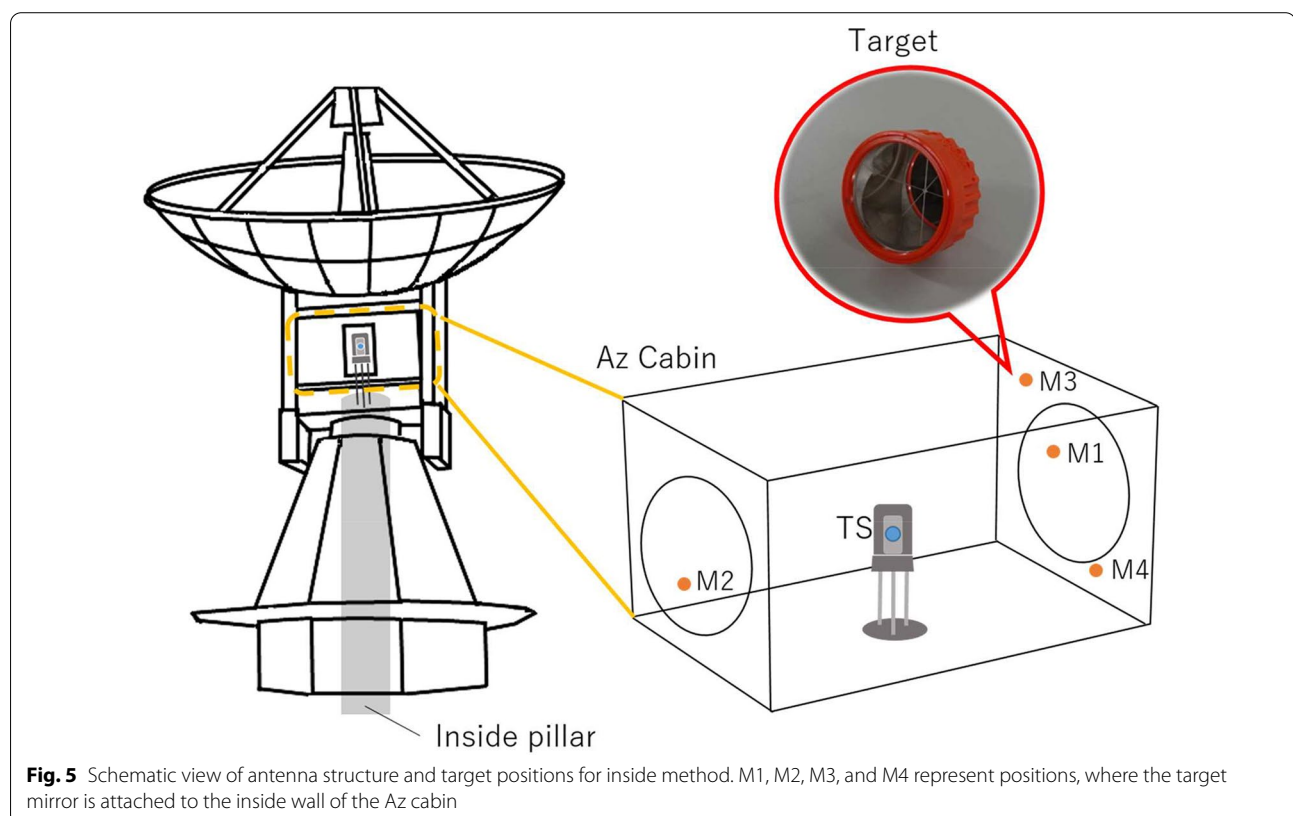
The procedure for the target observation in the inside method is as follows. We first determined the position of the inside pillar relative to Pillars 1 to 4 and VREF. We measured the distance and the angle from the inside pillar with a TS. Second, we observed the target mirror attached to the inside wall of the Az cabin at the inside pillar (Fig. 5). The TS was installed on the inside pillar, which is near the IVP position. We repeated the target observations for various Az or El directions as in
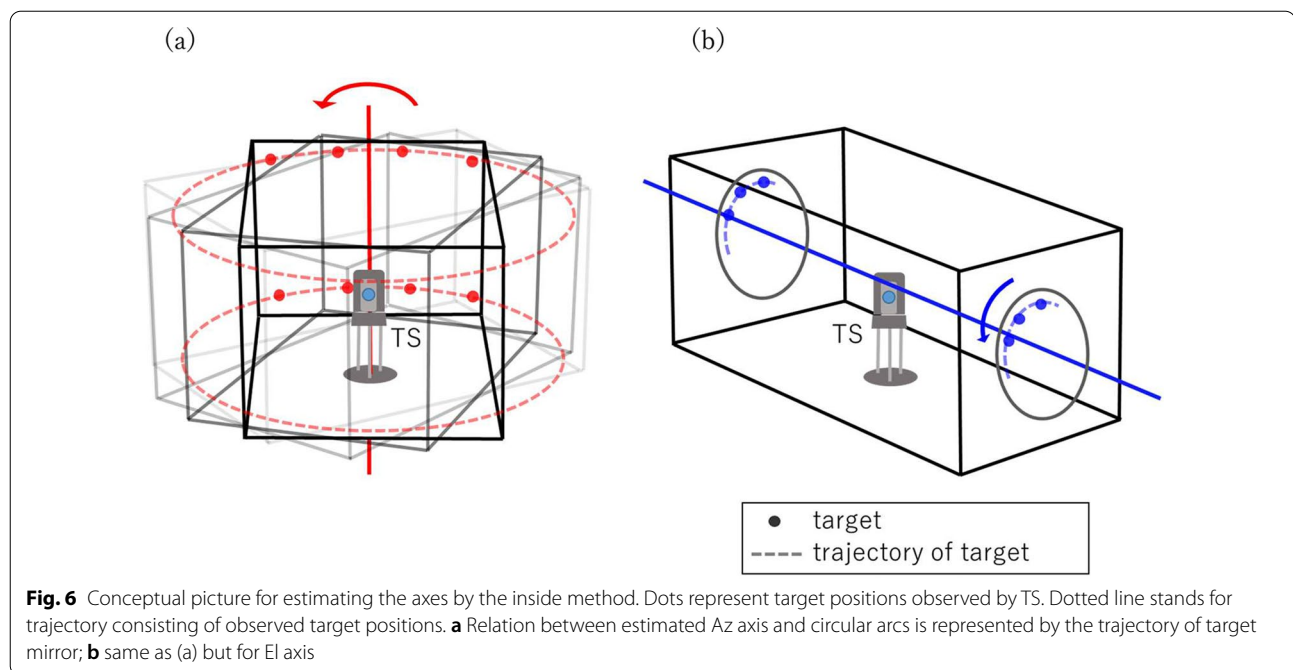
the outside method and collected the target positions (Fig. 6). The rotation axes were estimated using circular arcs consisting of observed target positions. The intersection of the estimated Az and El axes is the IVP.

Calculation

We used the software "pyaxis" to calculate the local-tie (Land Information New Zealand 2015). Input data are listed in Additional file 2: Table S2. Input data included the error values for each observation. In this study, the error values are in accordance with the rules given in Additional file 3: Table S3. Running the pyaxis software with the compiled observation data, we calculated the local-tie using the following three steps: (1) estimation of XYZ positions in the global frame for all observed points including the target mirror, the inside pillar, and Pillar 1 to 4 with the least squares adjustment; (2) estimation of the initial parameter for iteration, such as the positions of IVP and rotation axes using the positions calculated in step1; (3) re-estimation of XYZ positions, including the IVP using the parameters estimated in step 2 with the least squares adjustment.

Correction to the vertical deviation is also needed as an input value. The inclination of the geoid at the Ishioka station was calculated with the geoid value from the geoid model of Japan, "GSIGEO2011", provided by GSI

Fig. 5 Schematic view of antenna structure and target positions for inside method. M1, M2, M3, and M4 represent positions, where the target mirror is attached to the inside wall of the Az cabin

Matsumoto *et al. Earth, Planets and Space*   (2022) 74:147

Page 7 of 14

Fig. 6 Conceptual picture for estimating the axes by the inside method. Dots represent target positions observed by TS. Dotted line stands for trajectory consisting of observed target positions. **a** Relation between estimated Az axis and circular arcs is represented by the trajectory of target mirror; **b** same as (a) but for El axis

(Miyahara et al. 2014). We used the AUSPOS (Geoscience Australia 2000) provided by Geoscience Australia, which is the online GPS Processing Service to process the GNSS analysis (Jia et al. 2014).

Observation in 2018

We have conducted the co-location at Ishioka station to contribute for the construction of the ITRF regularly. In November 2018, we conducted the survey with the conventional outside method for the ITRF 2020 construction as part of the regular survey, while we additionally applied the inside method as a feasibility test to see if the inside method is applicable to the Ishioka's antenna. With this background, in current study, we used the data obtained by the two methods in 2018, and investigated the measurement accuracy. The main instruments we used for the observation are listed in Additional file 4: Table S4.

To observe with the outside method, we magnetically attached the target mirror (Leica Cateye-reflector) to the outside wall of the antenna and observed the target from two TSs (NET2B) installed on the neighboring pillars. Table 1 shows the observation sets. In the case of observation 1, we set the antenna at 0° in Az axis and 90° in El axis and observed the horizontal angle, vertical angle, and slope distance of the target from the Pillars 3 and 4. We repeated the process for 5 El angles at 1 Az direction and also for 8 directions in Az axis. We observed 40

points in total, excluding the outlier (observation 25) for the calculation.

For the observation with the inside method, we installed the targets (SOKKIA CPS12) on the wall inside the Az cabin. We used the TS to implement a utility to track the target automatically (NET05), while the antenna was rotating. We controlled the TS observation using a general mobile computer connected to the TS which could send commands to start/stop the observation and recorded the observed values as a log file. We got each value for horizontal/vertical angle and distance. There were 4 positions in which we installed the targets (Fig. 5); we recorded a total of 8 observations (Table 2). In the case of observation 3, the target was installed at M1, and the antenna was driven only for Az direction from 0° to 330° in El at 90°. We observed the target for every 30° of Az direction rotating clockwise and then counterclockwise. There were 4 set of observations for estimating the Az axis (Observation 3, 4, 7 and 8). We drew a circular arc with the track of targets for each observation set. We could estimate the Az axis as the line connecting the center points of these circles. In the case of El axis, two axes were estimated for Az 125° (Observation 1, 5) and Az 215° (Observation 2, 6) (Fig. 6).

For the estimation of the Az axis, we obtained 5 and 4 circular arcs using the outside and the inside method, respectively. The Az axis was determined as an optimal line connecting the centers of these circular arcs by the least squares method (Figs. 7a and 8a). We thus estimated one Az axis for both the methods. On the other hand, for the

Matsumoto *et al. Earth, Planets and Space*   (2022) 74:147

Page 8 of 14

Table 1 Combination of antenna's rotation angles and observation pillars for the outside method. The Az angle is measured from north clockwise, and the El angle is measured from horizon to zenith. Observation 25 is not used for the calculation due to outlier

Observation	Az [deg]	El [deg]	Observation point	Observation	Az [deg]	El [deg]	Observation point
1	0	90	Pillar 3 & Pillar 4	21	180	90	Pillar 1 & Pillar 2
2	0	60		22	180	60	
3	0	45		23	180	45	
4	0	30		24	180	30	
5	0	0		**25**	180	0	
6	335	0		26	165	0	
7	335	30		27	165	30	
8	335	45		28	165	45	
9	335	60		29	165	60	
10	335	90		30	165	90	
11	280	90	Pillar 2 & Pillar 3	31	95	90	Pillar 1 & Pillar 4
12	280	60		32	95	60	
13	280	45		33	95	45	
14	280	30		34	95	30	
15	280	0		35	95	0	
16	260	0		36	65	0	
17	260	30		37	65	30	
18	260	45		38	65	45	
19	260	60		39	65	60	
20	260	90		40	65	90	

Table 2 Combination of target mirror's positions and antenna rotation angles for inside method

Observation	Target position	Az [deg]	El [deg]
1	M1	125	0–90
2		215	0–90
3		0–330	90
4		0–330	0
5	M2	125	0–90
6		215	0–90
7	M3	0–330	90
8	M4	0–330	90

El axis, we estimated multiple axes. In the outside method, one El axis was estimated assuming that the target positions (derived from the measurements for 5 El angles) are positioned on a part of circular arc on a plane. In the 2018 observation, we obtained the 8 data sets for the estimation, as indicated by colored plots in Fig. 7b. In the inside method, we used the 2 data set for the estimation. One El axis was calculated using two circular arcs consisting of target positions which was measured at exact opposite Az directions. In the 2018 observation, we measured 4 Az angles, thus there are 2 pairs for the determination of El axis, as indicated by blue and light blue dots in Fig. 8b. We thus estimated one Az axis for both the methods, and 8 and 2 El axes for the outside method and the inside method, respectively.

Results and discussion

Local-tie determined by the outside and the inside methods

Table 3 shows the local-ties between VLBI and GNSS with the two methods. The VLBI–GNSS local-tie is represented as the geocentric orthogonal coordinate system (based on the ITRF2014, Epoch: 2018.316). The local-ties estimated by the inside method are shown in the upper column;

(See figure on next page.)
Fig. 7 Image of the estimated rotation axes and observed target positions for the outside method. **a** Az axis and target positions. Red-colored vertical line stands for the estimated Az axis. Red dots represent the observed target positions. Red-colored circles represent the trajectory of the target positions used for the estimate of Az axis; **b** El axes and target positions. Colored horizontal lines stand for the estimated El axes. Colored dots and circles represent the observed target positions and trajectory of the target positions, respectively
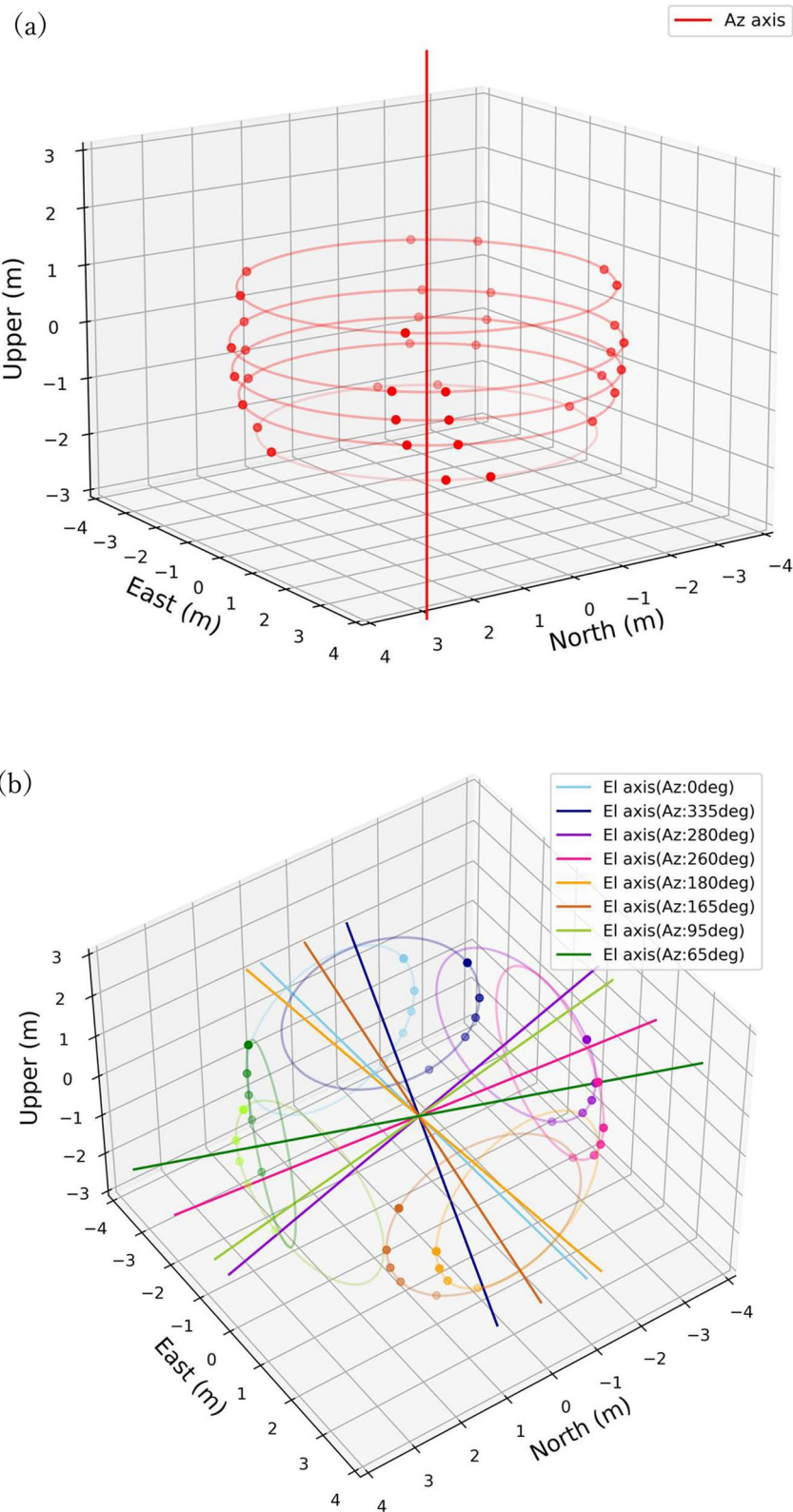
Matsumoto *et al. Earth, Planets and Space*   (2022) 74:147

Page 9 of 14

Fig. 7 (See legend on previous page.)

Matsumoto *et al. Earth, Planets and Space*   (2022) 74:147

Page 10 of 14

− 12.7395 m, 10.8621 m, and − 37.0959 m for X, Y, and Z, respectively, while, for the outside method, the estimated local-tie is − 12.7390 m, 10.8625 m, and − 37.0955 m for X, Y, and Z, respectively. The corresponding standard deviations are listed in parentheses; for the inside method, 0.9 mm, 0.9 mm, and 0.8 mm for X, Y and Z, respectively, and for the outside method, 0.8 mm, 0.7 mm, and 0.7 mm for X, Y, and Z, respectively. The striking point is that they both are less than 1 mm for each observation method, indicating that they meet the IERS criteria for measurement accuracy (Poyard 2017) in this case. We can conclude that both the observation methods achieve sufficient accuracy for estimating the IVP position.

We further emphasize that the differences in the IVP positions across the two observation methods are small; − 0.5 mm, − 0.4 mm, and − 0.4 mm for X, Y, and Z, respectively. It means that both the methods are capable of estimating almost the same position within a difference of less than 1 mm. We recognize that both methods can accurately determine the IVP position with the required accuracy in the common global frame.

Both the methods have comparable performance, while the inside method has a remarkable advantage, that is, the inside method substantially improves the efficiency of field work. It is obvious that working days for the inside method were less than those for the outside method. In the 2018 observation, it took 5 days in total to complete the measurement of the target for the outside method, while for the inside method it took only 1 day to complete. The major reason for the difference is the way of observation from pillars. For the outside method, we need to reinstall the TS on the other pillar when the target is no longer visible from a pillar after the antenna rotates around the Az axis. This is because the target mirror is attached to the antenna on one side (Fig. 4), and the target is not always visible from one place. One solution for improving the operational efficiency is the use of multiple TSs. In case of the 2018 co-location, we used two TSs for the target observation, thus spending 5 days to complete the target observation. However, the disadvantage is the high cost instruments. On the other hand, with the inside method, we can observe the targets at "one" place no matter where the mirror is attached in the Az cabin (Fig. 5). One TS is enough for the target observation. Reinstalling the TS is not required, and thus it is possible to observe many positions in a short time; only 1 day in the 2018 survey.

As suggested above, it is obvious that the inside method is accurate enough and is more efficient compared with the outside method. Therefore, we can say that the inside method is a more usable method than the outside method. Observation with the inside method is cost-effective, and the co-location can be conducted at short intervals for achieving continuous improvement of ITRF. We hope that the inside method would be widely used in future, although there are few stations which have the same type of antenna at the moment.

Comparison between axis method and sphere method

In addition to the way of estimating the IVP as an intersection of individual Az and El axes, described in Chapter 3, there is an alternative way to estimate the IVP using an imaginary sphere (Fig. 3b). We here call the former the "intersection of axes method (axis method)" (e.g., Dawson et al. 2005) and the latter the "center of imaginary sphere method (sphere method)" (e.g., Hasegawa et al. 2002). Calculation with the pyaxis is performed by the axis method. In the sphere method, the IVP is determined as the center of the imaginary sphere (Fig. 3b) which consists of observed target points. We had conventionally employed the sphere method to get the local-tie for submission to IERS (Matsuzaka et al. 2002), and also in the 2018 observation, we actually estimated the IVP by applying the sphere method in the 2018 observation. Therefore, we here compare the results calculated with the axis method and the sphere method to check the measurement accuracy.

The target positions are assumed to be on the surface of the imaginary sphere. The center position of the sphere is determined with the least squares method without the determination of Az/El axes (Miura et al. 2009). The detailed method is described in the Additional file 5: (Text S1).

We estimated the IVP using the same target points obtained by the outside method, and compared the results inferred from the axis method and the sphere method. Table 4 shows the local-tie and differences between the two. Upper column is the vector calculated by the sphere method, and the middle column is that by the axis method which is the same as the outside method shown in Table 3. The lower column stands for the

(See figure on next page.)
Fig. 8 Image of the estimated rotation axes and observed target positions for the inside method. **a** Az axis and target positions. Red-colored vertical line stands for the estimated Az axis. Red dots represent the observed target positions. Red-colored circles represent trajectory of the target positions, used for the estimate of the Az axis; **b** El axes and target positions. Blue and light blue-colored horizontal lines stand for the estimated El axes. Blue and light blue-colored dots and circles represent the observed target positions and trajectory of the target positions, respectively
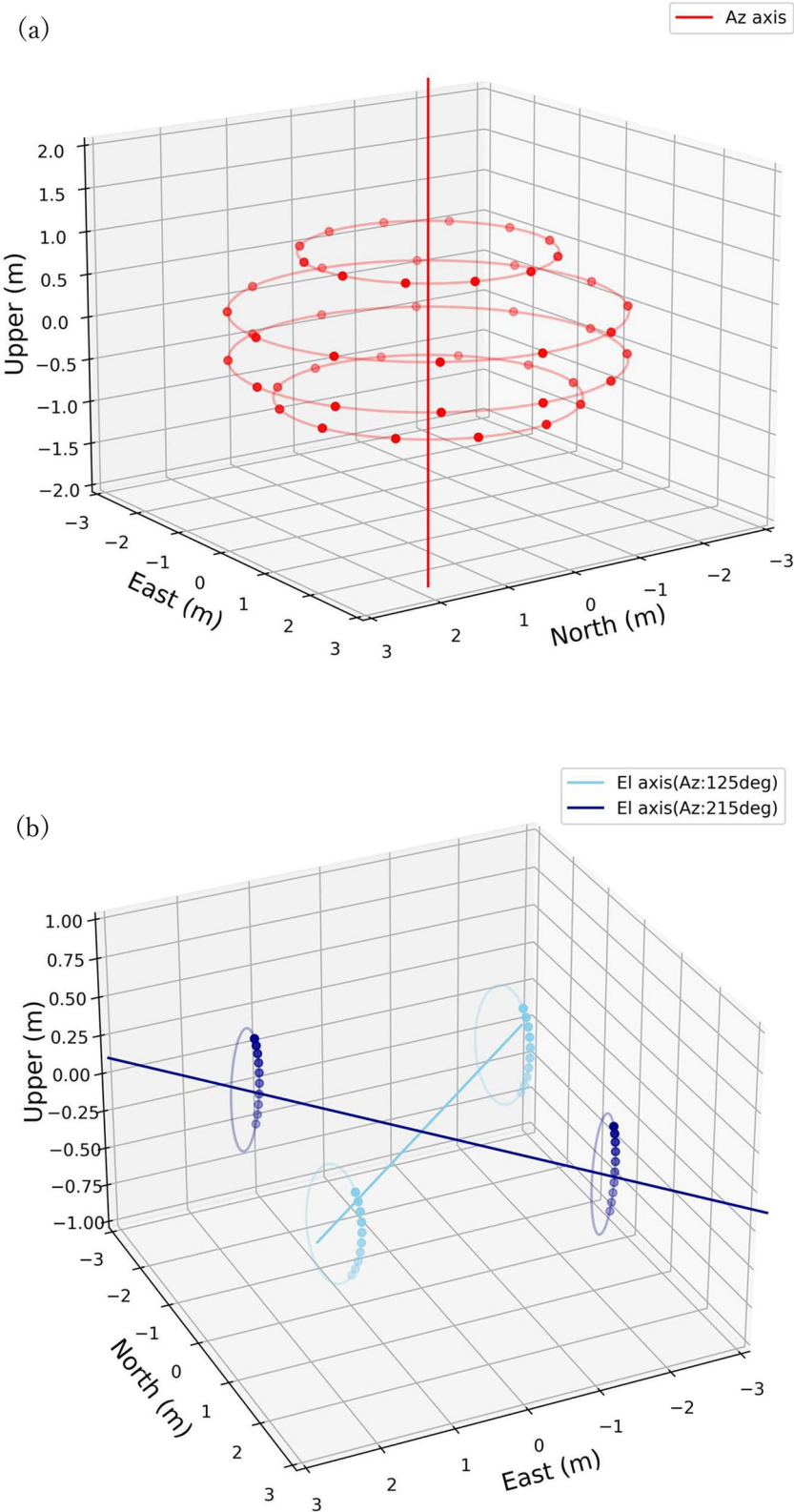
Matsumoto *et al. Earth, Planets and Space* (2022) 74:147

Page 11 of 14

Fig. 8 (See legend on previous page.)

Matsumoto *et al. Earth, Planets and Space*   (2022) 74:147

Page 12 of 14

Table 3 VLBI–GNSS local-tie vectors estimated by inside and outside methods. Values in parenthesis represent measurement errors

	X	Y	Z	Baseline
Inside method [m]	− 12.7395 (0.0009)	10.8621 (0.0009)	− 37.0959 (0.0008)	− 40.6987
Outside method [m]	− 12.7390 (0.0008)	10.8625 (0.0007)	− 37.0955 (0.0007)	− 40.6983
Differences [m]	− 0.0005	− 0.0004	− 0.0004	0.0004

Table 4 VLBI–GNSS local-tie vectors estimated by axes method and sphere method

	X	Y	Z	Baseline
Sphere method [m]	− 12.7390	10.8622	− 37.0960	40.6987
Axes method [m]	− 12.7390	10.8625	− 37.0955	40.6983
Differences [m]	0.0000	− 0.0003	− 0.0005	0.0004

Table 5 Offsets between Az and El axes estimated by the inside method and outside method

	El axis for antenna Az angle: [deg]	Offset [m]
Inside method	125	− 0.0001
	215	− 0.0001
	Average (abs.)	0.0001
Outside method	0	0.0007
	335	− 0.0002
	280	0.0004
	260	0.0024
	180	0.0014
	165	0.0044
	95	0.0009
	65	− 0.0016
	Average (abs.)	0.0015

difference in the IVP positions between the two methods. The differences are 0.0 mm, − 0.3 mm, and − 0.5 mm for X, Y, and Z, respectively, meaning that both methods can determine almost the same position. We here emphasize that both of the calculation methods are comparable to estimate the IVP with enough accuracy.

Although both of the methods can estimate the IVP position with comparable IVP accuracy, the axis method is preferable. This is because the offsets and orthogonality between Az and El axes, which is a parameter used as a kind of indicator to evaluate the mechanical accuracy of the antenna, can be calculated by determining the positions of the individual axes.

Here let us confirm how well the axes intersect actually. Table 5 shows the offsets estimated by the inside method and the outside method in the 2018 observation. For the inside method, the offset between the Az axis and the El axes is estimated to be 0.1 mm. For the

outside method, the offset is approximately 1.5 mm on an average, although the estimates have slight dispersion. There was little offset between the two axes, such that we could identify that the rotation axes of the Ishioka's antenna are not in skew position but almost intersect in the same plane.

Conclusions

We employed the inside and outside methods to determine the IVP position of the VLBI antenna in the 2018 co-location campaign at Ishioka station, and investigated the measurement accuracy in comparison with the estimated positions. Both the methods determined the IVP positions with a measurement error of less than 1 mm, which meets the criteria of measurement accuracy required by the IERS. It should be noted that the IVP positions are successfully estimated with a difference of less than 1 mm, suggesting that both the methods determine almost the same position independently. Either method can achieve a highly accurate estimate of the IVP position, while the inside method has an advantage in that the method substantially improves the operational efficiency. For the outside method, we need to repeat the target observations from four or more pillars around the VLBI antenna with reinstalling TS, while for the inside method, we can observe the target from one place inside the antenna in a short time with only one TS no matter where the target mirror is attached in the Az cabin. We can say that the inside method is an effective and practical approach to accurately estimate the IVP, although it is applicable to only the antenna having the specific structure containing the pillar inside. In addition, we compared the IVP positions estimated by two different calculation methods; the axis method and the sphere method. Both methods successfully determined almost the same IVP positions, with the differences of less than 1 mm. We can identify that both the methods can achieve enough measurement accuracy for IVP determination, while it would be desirable to use the axis method, because we can evaluate the mechanical accuracy of the antenna by utilizing the positional offset between the El and Az axes.

Matsumoto *et al. Earth, Planets and Space*   (2022) 74:147

Page 13 of 14

Abbreviations

ITRF: International Terrestrial Reference Frame; VLBI: Very Long Baseline Interferometry; IVP: Invariant point of VLBI antenna; IERS: International Earth Rotation and Reference Systems Service; TS: Total station; GGRF: Global Geodetic Reference Frame; GNSS: Global Navigation Satellite System; SLR: Satellite Laser Ranging; DORIS: Doppler Orbitography and Radiopositioning Integrated by Satellite; Ishioka: Ishioka Geodetic Observing Station; GSI: Geospatial Information Authority of Japan; VGOS: VLBI Global Observing System; IGS: International GNSS Service; CORS: IGS Continuously Operating Reference Station; DOMES: Directory Of MERIT Sites; ARP: Reference point of GNSS antenna; Az: Azimuth; El: Elevation.

Supplementary Information

The online version contains supplementary material available at https://doi.org/10.1186/s40623-022-01703-5.

Additional file 1: **Table S1** DOMES numbers.

Additional file 2: **Table S2** Input files for pyaxis.

Additional file 3: **Table S3** Error values for inputs to pyaxis.

Additional file 4: **Table S4** Main instruments.

Additional file 5: **Text S1** Detailed information of the observation by the outside method.

Additional file 6: **Figure S1** Observation set (left) and state of survey (right). (a) Traversing. (b) Leveling.

Additional file 7: **Figure S2** (a) Observation sets for traversing between GNSS and pillars. (b) Photograph of GNSS antenna. The target is installed under the antenna for traversing.

Additional file 8: **Figure S3** Survey for orientation angle. (a) Observation set; (b) light set to Mt. Tsukuba; (c) GNSS observation on Pillar 3 at Ishioka station.

Additional file 9: **Figure S4** Local frame used to the calculation by outside method.

Additional file 10: **Figure S5** Conceptual picture of vertical deviation.

Availability of data and materials

Geoid data are available at the following webpage: https://fgd.gsi.go.jp/download/menu.php

Declarations

Ethics approval and consent to participate

Not applicable.

Consent for publication

Not applicable.

Competing interests

The authors declare that they have no competing interests.

References

Altamimi Z, Rebischung P, Métivier L, Collilieux X (2016) ITRF2014: A new release of the international terrestrial reference frame modeling nonlinear station motions. J Geophys Res Solid Earth. https://doi.org/10.1002/2016JB013098

Altamimi Z, Rebischung P, Métivier L, Collilieux X (2017) Analysis and results of ITRF2014. IERS Technical Note; 38. Frankfurt am Main: Verlag des Bundesamts für Kartographie und Geodäsie, 76 pp. ISBN: 978–3–86482–088–5 (print version). https://www.iers.org/IERS/EN/Publications/TechnicalNotes/tn38.html-1.htm?nn=94912

Altamimi Z (2005) ITRF and co-location sites. In: Richter B, Schwegmann W, Dick R (eds) Proceedings of the IERS workshop on site co-location, Matera, Italy, 23–24 October 2003. IERS Technical Note; 33. Verlag des Bundesamts für Kartographie und Geodäsie, Frankfurt am Main, pp 8–15. ISBN: 3–89888–793–6 (print version). https://www.iers.org/IERS/EN/Publications/TechnicalNotes/tn33.html?nn=94912

Altamimi Z (2008) Importance of Local Ties for the ITRF. In: 13th FIG symposium on deformation measurement and analysis and 4th IAG symposium on geodesy for geotechnical and structural engineering, LNEC, LISBON, 12–15 May 2008. https://www.fig.net/resources/proceedings/2008/lisbon_2008_comm6/papers/pas02/pas02_01_altamimi_mc108.pdf

Dawson J, Johnston G, Twilley B (2005) The determination of telescope and antenna invariant point (IVP). In: Richter B, Schwegmann W, Dick WR (eds) Proceedings of the IERS workshop on site co-location, Matera, Italy, 23–24 October 2003. IERS Technical Note; 33. Verlag des Bundesamts für Kartographie und Geodäsie, Frankfurt am Main, pp 128–134. ISBN: 3–89888–793–6 (print version). https://www.iers.org/IERS/EN/Publications/TechnicalNotes/tn33.html?nn=94912

Geoscience Australia (GA) (2000) AUSPOS, http://www.ga.gov.au/scientific-topics/positioning-navigation/geodesy/auspos, Accessed 5 Feb 2022

Hasegawa H, Xia S, Tamura H, Ooizumi J, Yoshino T, Kunimori H, Amagai J, Katsuo F, Koyama Y, Kondoo T (2002) Methods of local survey between space geodetic observation systems at a collocation site. J Geodetic Soc Jpn 48(2):85–100

Jia M, Dawson J, Moore M (2014) AUSPOS: Geoscience Australia's on-line GPS positioning service. In: Proceedings of 27th international technical meeting of the satellite division of The institute of navigation (ION GNSS+ 2014), Tampa, Florida, September 2014, pp 315–320. https://www.ion.org/publications/abstract.cfm?articleID=12342

Land Information New Zealand (LINZ) (2015) pyaxis. https://github.com/linz/python-linz-pyaxis

López-Ramasco J, Córdoba-Hita B (2017) Local Tie Information Report Yebes Observatory, GUADALAJARA, Spain https://itrf.ign.fr/doc_ITRF/Report_Yebes_2016-063.pdf

Matsuzaka S, Hatanaka Y, Nemoto K, Fukuzaki Y, Kobayashi K, Abe K and Aiyama T (2002) VLBI-GPS Collocation method at geographical survey institute, IVS 2002 General Meeting Proceedings, p 96–100

Miura Y, Kurihara S, Yoshida K, Kawamoto S, Kotani K (2009) VLBI-GPS Colocation Survey, Bulletin of GSI (in Japanese), 119; 71–85. https://www.gsi.go.jp/common/000054739.pdf

Miyahara B, Kodama T, Kuroishi Y (2014) Development of new hybrid geoid model for Japan "GSIGEO2011." Bull Geosp Inf Auth Jpn 62:11–20

Petit G, Luzum B (eds) (2010) IERS Conventions (2010) IERS Technical Note; 36. Verlag des Bundesamts für Kartographie und Geodäsie, Frankfurt am Main, 2010. ISBN: 3-89888-989-6. https://www.iers.org/IERS/EN/Publications/TechnicalNotes/tn36.html-1.htm?nn=94912

Petrachenko B, Niell A, Behrend D, Corey B, Böhm J, Charlot P, Collioud A, Gipson J, Haas R, Hobiger T, Koyama Y, MacMillan D, Malkin Z, Nilsson T, Pany A, Tuccari G, Whitney A, Wresnik J (2009) Design aspects of

Matsumoto *et al. Earth, Planets and Space*   (2022) 74:147

Page 14 of 14

the VLBI2010 system. Progress report of the IVS VLBI2010 committee, NASA/TM-2009–214180, NASA Goddard Space Flight Center, Greenbelt, Maryland. https://ntrs.nasa.gov/archive/nasa/casi.ntrs.nasa.gov/20090034177.pdf

Poyard JC (2017) IGN best practice for surveying instrument reference points at ITRF co-location sites. IERS Technical Note; 39. Verlag des Bundesamts für Kartographie und Geodäsie, Frankfurt am Main. ISBN: 978–3–86482–129–5 (print version). https://www.iers.org/IERS/EN/Publications/TechnicalNotes/tn39.html?nn=94912

Rothacher M, Beutler G, Behrend D, Donnellan A, Hinderer J, Ma C, Noll C, Oberst J, Pearlman M, Plag HP, Richter B, Schöne T, Tavernier G, Woodworth PL (2009) The future global geodetic observing system. In: Plag HP, Pearlman M (eds) Global geodetic observing system. Springer, Berlin, Heidelberg. https://doi.org/10.1007/978-3-642-02687-4_9

Wessel P, Luis JF, Uieda L, Scharroo R, Wobbe F, Smith WHF, Tian D (2019) The generic mapping tools version 6. Geochem Geophys Geosyst 20:5556–5564. https://doi.org/10.1029/2019GC008515

Woods AR (2008) Indirect determination of the invariant reference point (IVP) of SLR and VLBI observing system. In: Joint symposia of 13th FIG Symposium on deformation measurement and analysis, 4th IAG Symposium on geodesy for geotechnical and structural engineering, LNEC, Lisbon, 12–15 May 2008. https://www.fig.net/resources/proceedings/2008/lisbon_2008_comm6/papers/pas02/pas02_03_wooods_mc066.pdf

Publisher's Note